

An ultrasensitive and low-cost graphene sensor based on layer-by-layer nano self-assembly

Cite as: Appl. Phys. Lett. **98**, 073116 (2011); <https://doi.org/10.1063/1.3557504>

Submitted: 01 January 2011 . Accepted: 31 January 2011 . Published Online: 18 February 2011

Bo Zhang, and Tianhong Cui



View Online



Export Citation

ARTICLES YOU MAY BE INTERESTED IN

[Graphene based piezoresistive pressure sensor](#)

Applied Physics Letters **102**, 161904 (2013); <https://doi.org/10.1063/1.4802799>

[Flexible room-temperature NO₂ gas sensors based on carbon nanotubes/reduced graphene hybrid films](#)

Applied Physics Letters **96**, 213105 (2010); <https://doi.org/10.1063/1.3432446>

[Ultra-sensitive strain sensors based on piezoresistive nanographene films](#)

Applied Physics Letters **101**, 063112 (2012); <https://doi.org/10.1063/1.4742331>

Lock-in Amplifiers up to 600 MHz

starting at

\$6,210



Zurich Instruments

Watch the Video

An ultrasensitive and low-cost graphene sensor based on layer-by-layer nano self-assembly

Bo Zhang and Tianhong Cui^{a)}

Department of Mechanical Engineering, University of Minnesota, 111 Church Street S.E., Minneapolis, Minnesota 55455, USA

(Received 1 January 2011; accepted 31 January 2011; published online 18 February 2011)

The flexible cancer sensor based on layer-by-layer self-assembled graphene reported in this letter demonstrates features including ultrahigh sensitivity and low cost due to graphene material properties in nature, self-assembly technique, and polyethylene terephthalate substrate. According to the conductance change of self-assembled graphene, the label free and labeled graphene sensors are capable of detecting very low concentrations of prostate specific antigen down to 4 fg/ml (0.11 fM) and 0.4 pg/ml (11 fM), respectively, which are three orders of magnitude lower than carbon nanotube sensors under the same conditions of design, manufacture, and measurement. © 2011 American Institute of Physics. [doi:10.1063/1.3557504]

Cancer marker has been elucidated as a powerful medical tool in disease prediction, diagnosis, and monitoring.¹⁻³ The clinical utility of protein biomarker to discriminate health and disease requires the capability to measure extremely low concentration proteins.⁴⁻⁶ The prevailing methods for detection of cancer markers include the enzyme linked immunosorbent assay,^{7,8} surface plasma resonance,⁹ microcantilevers,^{10,11} etc. Especially, nanomaterials, such as nanoparticle,¹²⁻¹⁵ carbon nanotube (CNT),^{16,17} and silicon nanowire,¹⁸ provide effective approaches for novel biosensors with better performance. However, a variety of methods demonstrate neither ultralow detection limits nor very large detection ranges,^{2,7-17} and many of them are incredibly expensive and complex to realize.^{9-11,19}

To overcome the hurdles of the previous detection methods, an ultrasensitive and low-cost biosensor based on layer-by-layer (LbL) self-assembled graphene is presented in this letter. Recently, graphene has attracted more and more attention due to its unique structural, electrical, chemical, and mechanical properties.²⁰ With rational physical and/or chemical modification, graphene is capable of detecting many types of molecules and ions.²¹⁻²⁵ Moreover, its inherently low electrical noise gives a very promising way to achieve very low detection limits.^{26,27} Therefore, using self-assembly of graphene on polyethylene terephthalate (PET), a flexible, low-cost, and label free cancer marker biosensor was synthesized for a real-time detection of prostate specific antigen (PSA) in a large detection range from 4 fg/ml to 4 μg/ml. In addition, a labeled PSA sensor was manufactured based on the same technique, which was also capable of a femtomolar detection. In comparison, a CNT based biosensor was characterized under the same design, fabrication, and measurement conditions in both label-free and labeled states, demonstrating that graphene was absolutely superior to CNT with respect to sensing detection limits. It was also confirmed by labeled normal rabbit immunoglobulin G (IgG) measurement results.

The cancer sensor reported herein was fabricated on a flexible PET substrate with lithographic patterned gold electrodes. 50/200 nm thick chromium/gold layers were depos-

ited on a clean PET wafer with an AJA sputter system (Model ATC 2000). Subsequently, sensor electrodes were patterned by photolithograph on a photoresist of 1 μm thick Shipley S1813 spin-coated at 3000 rpm for 30 s and exposed for 6 s. Another lithographic step was used to fabricate a window area on which the LbL graphene film was self-assembled and to protect the testing pads from the adsorption of graphene solutions. The polyelectrolytes used in this study were poly(diallyldiamine chloride) (PDDA) and poly(styrene sulfonate) (PSS), purchased from Sigma-Aldrich Inc. The concentrations of aqueous PDDA and PSS were 1.5 and 0.3 wt %, respectively, with an addition of 0.5 M sodium chloride to enhance the surface properties. Research grade graphene suspension solution (PureSheets™, 0.25 mg/ml) and carbon nanotube suspension solution (PureTube™, 0.25 mg/ml) were purchased from Nanointegris Inc. Next, the substrate was immersed into the charged suspensions with a sequence of [PDDA (10 min)+PSS (10 min)]₂ +[PDDA (10 min)+graphene suspension (20 min)]₅. The substrate was immersed into acetone for 5 min to lift off the photoresist, and the channel length and width of the LbL graphene composite were 20 and 500 μm, respectively. The same processes and patterns were adopted to fabricate CNT based biosensor. The thickness and resistance of five bilayers of self-assembled graphene film were 45 ± 5 nm and 0.9 ± 0.01 k Ω, characterized by surface profiler P16 and an Agilent data logger (34970A, Agilent Inc.), respectively. As shown in Fig. 1, the flexible biosensors were inspected by a scanning electron microscope (SEM) and an atom force microscope (AFM), presenting the defoliation of LbL self-assembled graphene. Subsequently, the biosensors were immunized by immobilization of anti-PSA on the surface with label-free and horseradish peroxidase (HRP) labeled methods, respectively. A graphene sensor was first immersed into 0.1% poly-L-lysine (Sigma-Aldrich Inc.) a solution for 1 h, followed by drying with a nitrogen stream. Next, the graphene sensor was incubated at 4 °C for overnight in PSA capture antibody solution (BioCheck Inc.) at a concentration of 10 μg/ml, prepared by a dilution into Dulbecco's phosphate buffered saline (PBS, Invitrogen Inc.). The sensor was rinsed with a PBS solution three times using a shaker (100 rpm, 19 mm circle) for 10 min each time. Next, the sensor

^{a)}Tel.: 612-626-1636. Electronic mail: tcui@me.umn.edu.

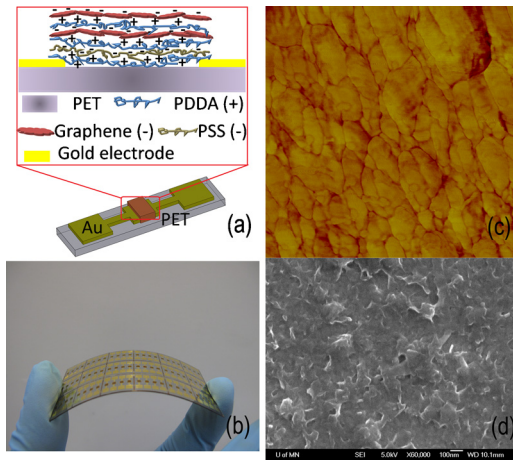


FIG. 1. (Color online) (a) Schematic illustration of LbL self-assembled graphene nanocomposite before immunization. (b) Optical image of LbL self-assembled graphene cancer sensor on a flexible PET substrate. (c) AFM image of LbL self-assembled graphene (scanning area is $1 \times 1 \mu\text{m}^2$). (d) SEM image of LbL self-assembled graphene displaying its porous defoliation surface profile. The average graphene nanoplatelet is about $100 \times 100 \text{ nm}^2$.

was incubated in a 3% bovine serum albumin (BSA, Sigma-Aldrich Inc.) blocking solution at room temperature for 5 h to block nonspecific binding sites. After repeating the rinsing step, the label-free sensor was ready for testing. Subsequently, the graphene biosensors were incubated in various concentrations of PSA (EMD Chemicals Inc.) for 1 h. Finally, after PSA sensors were incubated in HRP conjugated PSA secondary antibodies (BioCheck Inc., 255 ng/ml) for 1 h, the labeled sensors were ready for testing.

The detection principles of the biosensor are illustrated in Fig. 2. Given that the conductance of graphene is proportional to the product of charge carrier density and mobility, it is evident that changes in density and/or mobility of charge carriers must be responsive when molecules or ions are absorbed by graphene.²⁷⁻²⁹ The equation $\sigma = nqv$ can show the relationship clearly, where σ is the conductance, n is the carrier density, q is the charge per carrier, and v is the carrier mobility. In label free state [Fig. 2(a)], the conductance of the graphene based biosensor modified with the PSA capture antibody shifts with the concentration change of PSA solutions. In the labeled state [Fig. 2(b)], the HRP conjugated with PSA antibody catalyzes a biochemical reaction by the mixture of ascorbic acid and hydrogen peroxide. The con-

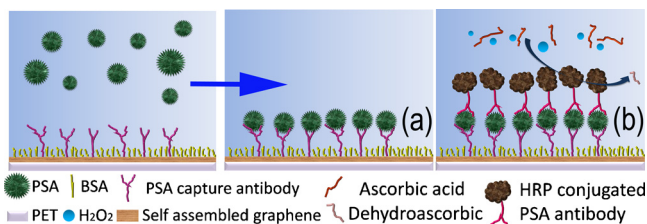


FIG. 2. (Color online) (a) Schematic illustration of interaction between capture antibodies and target protein molecules in a label-free detection. After graphene biosensor modified by capture antibodies encounters PSA solution, the immunoreaction will take place, and the conductance of graphene changes due to the absorption of PSA on the surface of the graphene. (b) Schematic illustration of a graphene sensor in a labeled detection. HRP labels the different concentrations of PSA and catalyzes the conversion from ascorbic acid to dehydroascorbic acid, causing the local pH shifts. The conductance of graphene is sensitive to pH shifts.

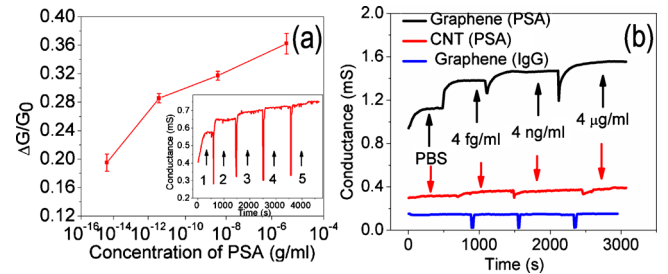


FIG. 3. (Color online) (a) Shift in normalized conductance vs PSA concentration for label-free graphene sensors. Inset: conductance vs time data recorded after alternate delivery of the following concentrations of PSA: (1) PBS contains no PSA, (2) 4 fg/ml, (3) 4 pg/ml, (4) 4 ng/ml, and (5) 4 $\mu\text{g/ml}$. Initial conductance G_0 represents the graphene conductance in PBS solution, and other conductance tested under different PSA concentrations subtract G_0 to get ΔG . (b) Conductance vs time testing for graphene and CNT biosensors with different PSA concentrations. The results demonstrate that the detection limit of graphene sensor is down to 4 fg/ml, compared with the CNT sensor with a detection limit of 4 ng/ml. In addition, various concentrations of normal rabbit IgG were delivered to the graphene sensor immunized with PSA capture antibodies, and the conductance of graphene sensor was kept constant.

ductance of the graphene biosensor varies with the local pH shifts.⁷

After LbL self-assembly of graphene, the PSA capture antibody was modified onto the graphene, and the sensor was blocked with BSA. Different concentrations of PSA diluted in PBS were introduced onto the label-free graphene sensor, and the conductance shift was monitored by the Agilent data logger. As shown in Fig. 3(a), the normalized conductance of graphene raises with the increase of PSA concentration from 4 fg/ml to 4 $\mu\text{g/ml}$. The conductance-versus-time measurements recorded on the graphene biosensor further confirm the trend in a real-time detection. The CNT sensor manufactured under the same conditions was conducted to compare with graphene sensors on the detection limits. As shown in Fig. 3(b), real-time results indicate that the CNT sensor is only capable of detecting PSA of 4 ng/ml, which is much less sensitive than the graphene sensor. The nonspecific reaction of normal rabbit IgG was implemented to further prove the specificity of this biosensor.

Electronic measurements of the graphene biosensor reveal its ultrahigh sensitivity, contributed by several facts. The critical property of graphene resulting in a very low detection limit is low 1/f noise due to the high quality of its crystal lattice and two-dimensional structures, which tend to screen charge fluctuations more than one-dimensional systems such as carbon nanotubes.^{26,27,30} In addition, the porous defoliation profile of self-assembled graphene promises more exposure to proteins, providing the greatest sensing area per unit volume.^{27,28}

Furthermore, the labeled cancer sensor was also tested to compare with the label-free one. After the HRP labeled immunization processes were executed, a mixture of 1 mM ascorbic acid (Sigma-Aldrich Inc.) and 1 mM o-phenylenediamine (Sigma-Aldrich Inc.) were produced with a dilution to PBS solution (1 mM Na-phosphate buffer, pH 6.0, with 15 mM NaCl). The role of o-phenylenediamine was to expedite the HRP catalyzed reaction. The conductance of graphene biosensor changes, as shown in Fig. 4(c), due to the local pH shift caused by the conversion of ascorbic acid into dehydroascorbic acid during the enzymatically catalyzed reduction.⁷ As shown in Fig. 4(a), the normalized

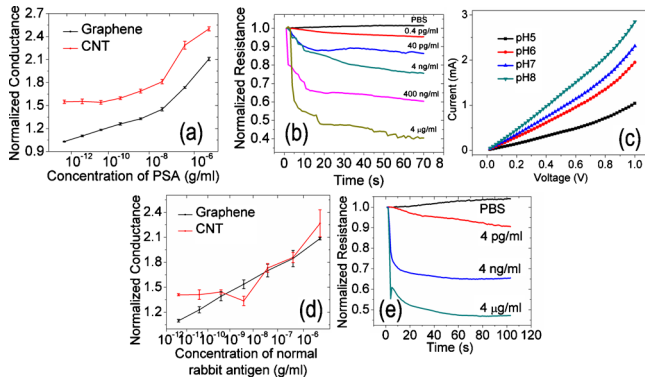


FIG. 4. (Color online) (a) Normalized conductance vs PSA concentration for labeled detection of graphene and CNT biosensors. The detection limit of graphene based sensors is 0.4 pg/ml, showing a great advantage over CNT sensors with a detection limit of only 4 ng/ml. Conductance was normalized by dividing the initial conductance in PBS without PSA. (b) Normalized resistance vs time recorded for labeled graphene sensor detection with different PSA concentrations. After incubated in various concentrations of PSA and labeled by HRP, shifts of graphene resistance were monitored when catalytic reaction started. Resistance was normalized through dividing the resistance after the mixture of ascorbic acid and hydrogen peroxide by the original resistance. (c) The conductance of the self-assembled graphene changes with the different local pH values. [(d) and (e)] Similar tests for the detection of normal rabbit antigen IgG. The detection limit of graphene sensors is 4 pg/ml, compared with the CNT sensors with a detection limit of only 40 ng/ml.

conductance of graphene raises with the increase of PSA concentration from 0.4 pg/ml to 4 μ g/ml, but the CNT sensor can only detect down to 4 ng/ml. As shown in Fig. 4(b), the normalized resistance of graphene changes with the PSA concentration. Due to the constitutive properties of graphene, the detection limit of the labeled biosensor is still better than other labeled detection methods.^{7,16,31,32} However, the labeled graphene sensor has a lower performance than the label-free sensor. The reasons are the following: First, the label free sensor allows the direct immunization reaction without an amplification implemented for signal sampling, which may easily induce a secondary electrical noise.^{7,18,33} Second, there is a 300 nm thick polymethylmethacrylate passivation layer on the labeled sensor, reducing the absorption of PSA.⁷

Although the PSA detection was used for a proof of protocol, this approach should be a generic platform for almost any target antigen with a known antibody. Similar experiment was performed for a detection of normal rabbit IgG with the immunization of goat anti-rabbit IgG, and it reconfirmed that the graphene sensor had a better performance than sensors with one-dimensional material CNT with respect to detection limits [Figs. 4(d) and 4(e)].

In summary, the LbL self-assembled graphene cancer sensor offers a number of advantages over the current protein detection techniques. Due to the low electronic noise, the porous defoliation profile, and the two-dimensional crystalline structure, the self-assembled graphene sensor presents an ultrahigh sensitivity. The detection limit and range of label free graphene sensors exceed most of the existing detection approaches.⁷⁻¹⁸ In addition, based on the LbL self-assembly technique and the PET substrate, the manufacture of graphene biosensors is much easier and is fully compatible with the standard microelectronic fabrication processes. Moreover, this detection platform can be extended to the

recognition of other antigens. This ultrasensitive, low-cost, and flexible cancer sensor may open a way to diagnose cancer and other complex diseases.

The authors acknowledge the assistance of fabrication and characterization from Nanofabrication Center and the Characterization Facility at the University of Minnesota. The authors also thank Dr. Min Zhang for his help in taking SEM images.

- ¹R. Etzioni, N. Urban, S. Ramsey, M. McIntosh, S. Schwartz, B. Reid, J. Radich, G. Anderson, and L. Hartwell, *Nat. Rev. Cancer* **3**, 243 (2003).
- ²H. Lilja, D. Ulmert, and A. J. Vickers, *Nat. Rev. Cancer* **8**, 268 (2008).
- ³Z. Zhong, W. Wu, D. Wang, D. Wang, J. Shan, Y. Qing, and Z. Zhang, *Biosens. Bioelectron.* **25**, 2379 (2010).
- ⁴J. Todd, B. Freese, A. Lu, D. Held, J. Morey, R. Livingston, and P. Goix, *Clin. Chem.* **53**, 1990 (2007).
- ⁵L. A. Tessler, J. G. Reifengerger, and R. D. Mitra, *Anal. Chem.* **81**, 7141 (2009).
- ⁶E. Stern, J. F. Klemic, D. A. Routenberg, P. N. Wyrembak, D. B. Turner-Evans, A. D. Hamilton, D. A. LaVan, T. M. Fahmy, and M. A. Reed, *Nature (London)* **445**, 519 (2007).
- ⁷M. Lu, D. Lee, W. Xue, and T. Cui, *Sens. Actuators, A* **150**, 280 (2009).
- ⁸M. Díaz-González, D. Hernández-Santos, M. B. González-García, and A. Costa-García, *Talanta* **65**, 565 (2005).
- ⁹C. Campagnolo, K. J. Meyersc, T. Ryand, R. C. Atkinson, Y. Chene, M. J. Scanlanf, G. Ritterf, L. J. Oldf, and C. A. Bat, *J. Biochem. Biophys. Methods* **61**, 283 (2004).
- ¹⁰G. Shekhawat, S. Tark, and V. P. Dravid, *Science* **311**, 1592 (2006).
- ¹¹M. Yue, J. C. Stachowiak, H. Lin, R. Datar, R. Cote, and A. Majumdar, *Nano Lett.* **8**, 520 (2008).
- ¹²J. Nam, C. S. Thaxton, and C. A. Mirkin, *Science* **301**, 1884 (2003).
- ¹³J. Zhang, L. Wang, D. Pan, S. Song, F. Boey, H. Zhang, and C. Fan, *Small* **4**, 1196 (2008).
- ¹⁴J. Zhang, L. Wang, H. Zhang, F. Boey, S. Song, and C. Fan, *Small* **6**, 201 (2010).
- ¹⁵J. Yan, S. Song, B. Li, Q. Zhang, Q. Huang, H. Zhang, and C. Fan, *Small* **6**, 2520 (2010).
- ¹⁶X. Yu, B. Munge, V. Patel, G. Jensen, A. Bhirde, J. D. Gong, S. N. Kim, J. Gillespie, J. S. Gutkind, F. Papadimitrakopoulos, and J. F. Rusling, *J. Am. Chem. Soc.* **128**, 11199 (2006).
- ¹⁷W. Xue and T. Cui, *Sens. Actuators B* **134**, 981 (2008).
- ¹⁸G. Zheng, F. Patolsky, Y. Cui, W. U. Wang, and C. M. Lieber, *Nat. Biotechnol.* **23**, 1294 (2005).
- ¹⁹J. Choi, B. Oh, Y. Jang, and D. Kang, *Appl. Phys. Lett.* **93**, 033110 (2008).
- ²⁰K. S. Novoselov, A. K. Geim, S. V. Morozov, D. Jiang, Y. Zhang, S. V. Dubonos, I. V. Grigorieva, and A. A. Firsov, *Science* **306**, 666 (2004).
- ²¹Y. Ohno, K. Maehashi, Y. Yamashiro, and K. Matsumoto, *Nano Lett.* **9**, 3318 (2009).
- ²²S. He, B. Song, D. Li, C. Zhu, W. Qi, Y. Wen, L. Wang, S. Song, H. Fang, and C. Fan, *Adv. Funct. Mater.* **20**, 453 (2010).
- ²³Q. He, H. G. Sudibya, Z. Yin, S. Wu, H. Li, F. Boey, W. Huang, P. Chen, and H. Zhang, *ACS Nano* **4**, 3201 (2010).
- ²⁴Z. Wang, X. Zhou, J. Zhang, F. Boey, and H. Zhang, *J. Phys. Chem. C* **113**, 14071 (2009).
- ²⁵X. Zhou, Y. Wei, Q. He, F. Boey, Q. Zhang, and H. Zhang, *Chem. Commun. (Cambridge)* **2010**, 6974.
- ²⁶J. T. Robinson, F. K. Perkins, E. S. Snow, Z. Wei, and P. E. Sheehan, *Nano Lett.* **8**, 3137 (2008).
- ²⁷K. Ratnac, W. Yang, S. Ringer, and F. Braet, *Environ. Sci. Technol.* **44**, 1167 (2010).
- ²⁸F. Schedin, A. K. Geim, S. V. Morozov, E. W. Hill, P. Blake, M. I. Katsnelson, and K. S. Novoselov, *Nature Mater.* **6**, 652 (2007).
- ²⁹E. H. Hwang, S. Adam, and S. Das Sarma, *Phys. Rev. B* **76**, 195421 (2007).
- ³⁰Y. Lin and P. Avouris, *Nano Lett.* **8**, 2119 (2008).
- ³¹B. V. Chikkaveeraiah, A. Bhirde, R. Malhotra, V. Patel, J. S. Gutkind, and J. F. Rusling, *Anal. Chem.* **81**, 9129 (2009).
- ³²N. V. Panini, G. A. Messina, E. Salinas, H. Fernandez, and J. Raba, *Biosens. Bioelectron.* **23**, 1145 (2008).
- ³³J. Lee, Z. Wang, J. Liu, and Y. Lu, *J. Am. Chem. Soc.* **130**, 14217 (2008).